Published in final edited form as:
Diabetologia. 2010 January ; 53(1): 160–169. doi:10.1007/s00125-009-1553-y.

Diabetes regulates mitochondrial biogenesis and fission in neurons

J.L. Edwards[1], **A. Quattrini**[2], **S.I. Lentz**[3], **C. Figueroa-Romero**[1], **F. Cerri**[2], **C. Backus**[1], **Y. Hong**[1], and **E.L. Feldman**[1,4]

[1]Department of Neurology, The University of Michigan, Ann Arbor, Michigan, U.S.A.

[2]Department of Neurology and INSPE San Raffaele Scientific Institute, Milan, Italy

[3]Department of Internal Medicine, Division of Metabolism, Endocrinology and Diabetes, The University of Michigan, Ann Arbor, Michigan, U.S.A.

[4]A. Alfred Taubman Medical Research Institute, The University of Michigan, Ann Arbor, Michigan, U.S.A.

Abstract

Aims—Normal mitochondrial (Mt) activity is a critical component of neuronal metabolism and function. Disruption of Mt activity by altered Mt fission and fusion is the root cause of both neurodegenerative disorders and Charcot-Marie-Tooth Type 2A inherited neuropathy. The current study addressed the role of Mt fission in the pathogenesis of diabetic neuropathy (DN).

Methods—Mt biogenesis and fission were assayed in both *in vivo* and *in vitro* models of DN. Gene, protein, mitochondrial DNA and ultrastructural analyses were used to assess Mt biogenesis and fission.

Results—Our data reveal increased Mt biogenesis in dorsal root ganglion (DRG) neurons from diabetic compared to non-diabetic mice. An essential step in Mt biogenesis is Mt fission, regulated by the Mt fission protein Drp1. Evaluation of *in vivo* diabetic neurons indicated small, fragmented Mt, suggesting increased fission. *In vitro* studies reveal short-term hyperglycemic exposure increased expression of Drp1. The influence of hyperglycemia-mediated Mt fission on cellular viability was evaluated by knockdown of Drp1. Knockdown of Drp1 resulted in decreased susceptibility to hyperglycemic damage.

Conclusions—We propose that: 1) Mt undergo biogenesis in response to hyperglycemia, but the increased biogenesis is insufficient to accommodate the metabolic load; 2) hyperglycemia causes an excess of Mt fission, creating small, damaged mitochondria; and 3) reduction of aberrant Mt fission increases neuronal survival and indicates an important role for the fission-fusion equilibrium in the pathogenesis of DN.

Address correspondence to: Eva L. Feldman M.D., Ph.D., University of Michigan, Department of Neurology, 5017 BSRB, 109 Zina Pitcher Place, Ann Arbor, MI 48109, Phone: (734) 763-7274, Fax: (734) 763-7275, efeldman@med.umich.edu.

Duality of interest The authors declare that there is no duality of interest associated with this manuscript.

Keywords

Diabetic Neuropathy; Mitochondrial Biogenesis; Mitochondrial Fission

Introduction

Mitochondrial (Mt) damage is central to the pathophysiology of both inherited and acquired neuropathies [1, 2]. In diabetic neuropathy (DN), physiological abnormalities of sensory neurons are directly initiated by hyperglycemia [1, 3], though subsequent mechanisms leading to neuronal dysfunction are not fully characterized. Our laboratory has demonstrated the critical role of Mt in the progression of hyperglycemia-mediated neuronal damage [4]. *In vitro* models of DN reveal that hyperglycemia overwhelms normal Mt function in dorsal root ganglion (DRG) neurons, resulting in the production of reactive oxygen species (ROS). ROS in turn damage the Mt electron transport apparatus and cellular proteins, lipids, and DNA. Mt membrane depolarization and the loss of ATP production, in particular, precede neuronal dysfunction [5, 6]. In parallel, DRG neurons from *in vivo* rodent models of DN contain vacuolated Mt with disrupted cristae [7] with biochemical evidence of ROS [7].

Mt networks are dynamic, undergoing both Mt biogenesis and Mt fission [8]. The distinction between Mt biogenesis and fission is based on whether or not there is replication of MtDNA and an increase in Mt mass. By definition, Mt biogenesis involves complete MtDNA replication. In contrast, fission occurs in the absence of MtDNA replication, and the existing copies of MtDNA are simply divided between the new “fissioned” Mt [8, 9]. Thus Mt networks are dynamic and respond to metabolic signals by increasing the actual mass of the network (biogenesis) as well as dispersing the existing Mt into a larger network (fission).

Increased Mt biogenesis is part of the cellular response to oxidative stress [10]. Mt biogenesis attenuates oxidative stress by increasing Mt capacity to metabolize reducing equivalents. Cells undergoing Mt biogenesis consume less oxygen, maintain Mt membrane potential, and produce fewer ROS, which together decrease cellular damage and increase survival [11, 12]. Neurons transfected with the Mt biogenesis-promoting protein peroxisome proliferator activated receptor-coactivator alpha (PGC-1α) are protected against paraquat- or H_2O_2-induced oxidative stress [13]. Despite the neuroprotective effects of Mt biogenesis, its role in DN is not well characterized. Current theory suggests that increased Mt biogenesis allows cells to accommodate increased energy loads, thereby promoting cellular viability [14].

While Mt biogenesis increases Mt mass, Mt fission increases the actual number of Mt. Drp1 is a GTPase that translocates from the cytosol to the outer Mt membrane to mediate Mt fission at sites known as Mt scission sites [15, 16]. Fis1is anchored to the outer Mt membrane and promotes fission in concert with Drp1 [17-19].

Previous work in our laboratory has implicated Drp1 in hyperglycemia-mediated Mt damage in sensory neurons [1]. We contend that Mt initially attempt to disperse the metabolic load of prolonged hyperglycemia by maintaining a dynamic balance between Mt biogenesis and fission. We hypothesize that Mt networks are disrupted as ROS accumulate with loss of

ATP generation and excessive Mt fission, producing unstable Mt networks and neural injury. As a first step to test this hypothesis, the current study examined the role of Mt biogenesis and fission in hyperglycemia-induced neuronal damage using *in vivo* and *in vitro* models of DN. We detected increased levels of MtDNA and biogenesis related proteins in DRG neurons from a genetic murine model of type 2 diabetes with DN; however, these Mt were significantly smaller and more electron dense. The presence of small, fragmented Mt and increased levels of Drp1 suggested increased Mt fission and was investigated further *in vitro*. Because Drp1 is essential for both Mt fission and cell viability, we hypothesized that attenuation of Drp1 levels would decrease Mt fission and improve short term neuronal survival. Efficient knockdown of Drp1 in DRG neurons decreased glucose-mediated neuronal injury. Our data suggest that an imbalance in Mt neural networks favoring Mt fission in DRG neurons plays a role in the pathogenesis of DN and suggests that therapies that maintain Mt neural networks could be beneficial in the treatment of DN.

Methods

Diabetic Mice

Diabetic (BKS.Cg-*m+/+Lepr*^{db}, BKS-db/db) and control (BKS-db/+) mice were purchased from Jackson Laboratories (Bar Harbor, Maine). Mice were housed in a pathogen-free environment with continuous access to food (Purina 5053 chow) and water on a 12 h light-dark schedule, and cared for following the University of Michigan Committee on the Care and Use of Animals guidelines (approval #07675) [20].

At the end of the experimental period, glycated hemoglobin (GHb) was measured using the Helena Laboratories Test Kit, Glyco-Tek Affinity Column Method. Analyses and procedures were performed in compliance with established AMDCC protocols (http://www.amdcc.org). At the 5 week time point (n = 9 for each group), the BKS-db/+ and BKSdb/db had an average weight of 18.5 vs 23.5 g and a glycated hemoglobin of 4.3% vs 5.3%; at 24 weeks, comparing BKS-db/+ to BKSdb/db, weights were 26.5 g vs 52.2 g with glycated hemoglobins of 7.6% vs 13.0%.

DRG were harvested at 5 and 24 weeks of age (1 and 20 weeks of diabetes). The mice were euthanized by sodium pentobarbital overdose. A blood sample (50 μL) was collected for measurement of GHb (see above). DRG were harvested by microdissection, immediately immersed in liquid nitrogen, and stored at −70°C. Protein was extracted using T-PER tissue protein extraction reagent (Pierce, Rockford IL).

Embryonic DRG culture

Dissociated DRG neurons were isolated from E15 Sprague Dawley rat embryos and plated in NB+ media supplemented with B27 (without antioxidants) and 1.4 mM L-glutamine. NB + media was composed of Neurobasal media + 30nM selenium, 10nM hydrocortisone, 10μg/mL transferrin, 10nM β-estradiol, 10ng/mL 2.5S nerve growth factor, 7μM aphidicolin, and penicillin/streptomycin/neomycin (5,000 U/5 mg/10 mg per mL, respectively). After 24 h, cultures were re-fed with fresh NB+ without B-27 or L-glutamine. Cultures were used for experiments after 3 d, at which time > 95% of the cells were neurons.

NB+ media contained 25 mM glucose (control medium), which is optimal for DRG neuronal survival and neurite outgrowth [7]. High glucose treatment media consisted of control media plus 20 mM additional glucose for a final concentration of 45 mM glucose. This parallels the 1.4-fold increase in blood glucose concentration found in human patients with diabetes [21].

In Vitro Incorporation and Visualization of BrdU into MtDNA

Cultures were prepared as above and plated on 25 μg/ml laminin-coated glass coverslips. Two days after plating, neurons were incubated with 15 μM bromodeoxyuridine (BrdU, Sigma) for 6 h. Cells were fixed with 2% paraformaldehyde, permeabilized with 0.1% Triton X-100 for 10 min at RT, and DNA denatured with 2N HCl for 30 min at 37°C. Immunocytochemistry was performed by incubating with anti-BrdU (Vector Labs) at 1:50 overnight at 4°C. BrdU signal was amplified using a HRP-goat anti-mouse antibody and AlexaFluor488 tyramide signal amplification (TSA) kit (Invitrogen) following the manufacturer's protocol. Coverslips were mounted with Prolong Gold containing DAPI (Invitrogen).

An Olympus FluoView500 confocal microscope was used to image fluorescent signals with a 60× oil objective and magnified 2× with FluoView software (v5.0). Fluorescent signals were sequentially scanned at z-intervals of 0.225 μm. Maximum projections of the 3D data were used to show BrdU incorporation in MtDNA of representative neurons. Analysis of BrdU labeled MtDNA was done with Volocity software (v4.2, Improvision, Waltham, MA). Z-series were deconvolved with fast restoration and cropped to isolate individual neurons. BrdU labeled MtDNA were classified by: fill holes in objects, separate touching objects by 0.1 nm and exclude objects by size (0.008 -0.5 nm). The number of BrdU positive MtDNA was counted per DRG soma.

Transmission electron microscopy (TEM)

Semi-thin and ultra-thin morphological analyses were performed as described [22]. Age-matched BKS-db/db and db/+ mice were euthanized as described above and perfused with 4% paraformaldehyde in phosphate buffered saline (0.1 M, pH 7.2). DRGs were removed and post-fixed in 0.12 M phosphate buffer containing 2% glutaraldehyde. DRGs were post-fixed with osmium tetroxide, and embedded in Epon (Fluka, Buchs SG, Switzerland). Ultra-thin sections (100–120 nm thick) were stained with uranyl acetate and lead citrate and examined by TEM. All ultrastructural analyses were performed in a blinded and nonbiased manner from photomicrographs (magnification × 8,000: db/db 41, db/+ 42 photographs) using a Zeiss Leo 912 transmission electron microscope (Omega, Brattleboro, VT). An average of 20 neurons per mouse was analyzed. Each image represents a 7.5-μm^2 region of the cytoplasm. Cross sections were randomly selected for analysis from BKS-db/db (n = 2) and db/+ (n = 2) mice. Mt density (#Mt/area) and diameter were assessed.

miRNA knockdown of Drp1

Lentivirus containing miRNA for human and mouse Drp1 in the pGIPz vector (Open Biosystems, Huntsville, AL) were produced through the University of Michigan Vector Core (http://www.med.umich.edu/vcore/). DRG neurons were infected with a 1× stock of

virus on the day of plating, and media changed from NB+ supplemented with B-27 and L-glutamine to NB+ without B-27, L-glutamine, and virus 1 d after plating/infection [1]. All viral infections were performed in accordance with the University of Michigan Institutional Biosafety Committee guidelines.

Immunoblotting

Protein levels were determined using Western immunoblotting on whole cell lysates from both *in vivo* (described above) and *in vitro* DRG. DRG neurons were cultured as described above in 60 mm Biocoat collagen coated plates (BD Biosciences). Neurons were exposed to control (25 mM) or high glucose (45 mM) media for 0 or 6 h, and prepared for Western blotting per our published protocol [23]. Equivalent amounts of protein were subjected to 12.5% SDS-PAGE and transferred to PVDF (Pall, East Hills, NY). PVDF membranes were probed using antibodies against COX-IV (Invitrogen), PGC1-α (Cayman Chemical, Ann Arbor, MI), Drp1 (Abnova Corp., Walnut, CA), cleaved Caspase-3 (Cell Signaling, Danvers, MA) and actin (SantaCruz Biotechnology, Santa Cruz, CA) used at 1:1000 dilution. Blots were developed using enhanced chemiluminescence and densitometry was performed with data normalized to actin [24].

Mitochondrial DNA Quantitation

DNA was extracted using the Genelute Mammalian Genomic DNA Kit (Sigma) according to the manufacturer's instructions. Real-time PCR amplification and SYBR Green fluorescence detection were performed using the iCycler iQ Real-time Detection system (Bio-Rad, Hercules, CA). The fluorescence threshold (C_T) value was calculated by the iCycler iQ system software. MtDNA levels were quantitated by normalizing the mitochondrial gene (cytochrome b) to the nuclear gene (glyceraldehyde-3-phosphate dehydrogenase, GAPDH). The $2^{-\Delta\Delta CT}$ method was used. A total of 10 ng genomic DNA was used for MtDNA and nuclear DNA markers, in a 25 μL reaction containing 1X SYBR Green iCycler iQ mixture and 0.2 μM each of forward and reverse gene-specific primers. Primer sequences are listed in Table 1.

RNA Isolation and Real-Time PCR

Total RNA was extracted using an RNeasy Kit (Qiagen, Valencia, CA) according to the manufacturer's instructions. Reverse transcription was performed using iScript cDNA Synthesis kit (Bio-Rad). Real-time PCR reactions were carried out in 96-well 0.2 ml PCR plates sealed with iCycler Optical Sealing tapes (Bio-Rad). Sequence information of all the primers is listed in Table 2. The PCR amplification profile was: 95°C for 5 min, 40 cycles of denaturation at 95°C for 30 s, annealing at 58°C for 1 min, extension at 72°C for 30 s and a final phase of 72°C for 5 min. The fluorescence threshold $C_T$value was calculated by the iCycler iQ system software and the levels were first normalized to the endogenous reference GAPDH (ΔC_T), then relative to the control group ($\Delta\Delta C_T$) and expressed as $2^{-\Delta\Delta CT}$. PCR product levels were demonstrated as mean ± SEM and a two-sample equal variance t-test was performed (n = 4 mice per condition).

Results

Mitochondrial biogenesis is altered by hyperglycemia in vivo

Diabetes results in significant disruption of Mt structure and function [4, 7, 25] and regulates multiple genes related to Mt metabolism and biogenesis [26] in DRG neurons. These observations were extended by examining Mt biogenesis in mice with DN. To avoid the potential confounding affects of streptozotocin [27], we examined a genetic model of type 2 diabetes that exhibits profound DN [20, 28].

MtDNA replication is a necessary component of Mt biogenesis and a commonly used marker for Mt biogenesis [29]. MtDNA was measured in DRG harvested from BKS-db/db and db/+ mice at 5 and 24 weeks of age (1 and 20 weeks of diabetes). In Figure 1, MtDNA levels in DRG harvested at 5 weeks revealed no significant differences between BKS-db/db and db/+ mice. In contrast, 24 week old BKS-db/db DRG contained twice the relative amount of MtDNA as age-matched db/+ DRG.

The expression of six genes related to Mt biogenesis was examined at the levels of transcription and translation in DRG harvested from BKS-db/db and db/+ mice. These genes include the Mt fission proteins Drp1 and Fis1, which form complexes on the outer Mt membrane; the Mt fusion protein MFN2; the MtDNA-encoded protein COX-IV (OxPhos Complex IV subunit I), a marker of Mt mass; the Mt biogenesis protein PGC1-α (involved in glucose metabolism); and PGC1-β involved in lipid metabolism [30] and an internal control (GAPDH). At 5 weeks, Fis1 and PGC1-α were significantly elevated ($p<0.05$) in the DRG harvested from BKS-db/db neurons compared to the db/+ (Figure 2). At 24 weeks, COX-IV and PGC1-α were elevated in DRG compared to 5 week old mice, but were not regulated by diabetes (Figure 2). These data suggest that transcription of Fis1 and PGC1-α is altered as an acute response to hyperglycemia, but not to a prolonged hyperglycemia.

Interestingly, analysis of protein expression indicates that at 5 weeks, BKS-db/db and db/+ DRG exhibit no significant differences in PGC1-α, COX-IV, and Drp1 (Figure 3A). In contrast, DRG from 24 week-old BKS-db/db DRG demonstrated a 55% increase of PGC1-α, a 34% increase in COX-IV, and 21% increase in Drp1 compared to db/+ DRG (Figure 3B). An increase in protein levels suggests the presence of Mt biogenesis in diabetic (db/db) mice. To ensure that Mt biogenesis was not ubiquitous throughout the BKS-db/db animal, skeletal muscle from 24 week-old BKS-db/db and db/+ mice were analyzed and demonstrated no changes in Drp1 or COX-IV (data not shown).

Prolonged hyperglycemia leads to an increase in Mt fission

Mt localized within DRG cell bodies from BKS-db/db mice differed morphologically from db/+ Mt. Mt from BKS-db/+ mice displayed normal, round morphology with discrete cristae and a contiguous matrix (Figure 4A). In contrast, Mt of BKS-db/db mice appeared smaller, fragmented and asymmetric (Figure 4B-D). Mt membrane density and cristae structure were also altered. Mt from BKS-db/db neurons showed signs of the inner membrane enclosing itself to form individual compartments. Based on the classification system by Sun et al., Mt from the BKS-db/db are characterized as normal-vesicular and vesicular[31]. Further structural analysis of the diabetic Mt indicated an energized state (activity in electron

transport chain complexes) with dilated intercristae spaces and increased matrix density (Figure 4D).

A quantitative evaluation of Mt in randomly selected DRG neurons from 24 week-old BKS-db/db and db/+ mice (Figure 4) detected an increase in Mt density (BKS-db/db 1.283 ± 0.06 Mt/μm^2 vs. db/+ 0.9138 ± 0.05 Mt/μm^2 $p<0.0001$; Figure 4E). Mt from BKS-db/db mice exhibited reduced diameters compared with db/+ (219.6 ± 3.3 nm vs. 292.4 ± 5.8 nm; *n Mt* = 404-281; $p<0.0001$; Figure 4E). These results indicate prolonged hyperglycemia alters Mt dynamics as well as morphology *in vivo*.

Hyperglycemia increases mitochondrial biogenesis and fission in DRG neurons in vitro

To further investigate hyperglycemia-induced Mt biogenesis, we examined DRG neurons under hyperglycemic *in vitro* conditions and assessed MtDNA replication and protein expression. Dissociated DRG neurons were incubated in control (25 mM) and high glucose (45 mM) media for 6 h and MtDNA was quantified (Figure 5). A two-fold increase in cytochrome b DNA was detected in DNA isolated from DRG neurons grown in high glucose compared to control media (Figure 5A). MtDNA replication was also measured in individual DRG neurons by BrdU incorporation. DRG neurons exposed to high glucose for 6 h showed an increase in number of MtDNA labeled with BrdU (Figure 5B). The increase in BrdU positive MtDNA in individual DRG neurons treated with high glucose was comparable to the increase measured by isolated DNA (Figure 5C). Mt COX-IV protein levels were not changed following exposure to high glucose; however, there was an increase in Drp1 levels (Figure 5D) in agreement with our previous studies [1]. Increased expression of Drp1 suggests increased Mt fission, while stable COX-IV expression suggests no increase in Mt mass. Together, these findings suggest that incomplete Mt biogenesis or an over-activity of Mt fission occurs during short-term hyperglycemia.

Mt fission may either promote or diminish the viability of stressed cells [32, 33]. To investigate the role of Mt fission on cell viability under hyperglycemic conditions, Drp1 expression was decreased via lentivirus-administered miRNA (Figure 6). Infection of DRG neurons with mouse anti-Drp1 miRNA constructs achieved a knockdown of Drp1 levels compared to uninfected neurons cultured in low glucose media. Scrambled (non-specific) miRNA had no significant effect on Drp1 levels. Cleaved Caspase-3 (casp3) was used to evaluate cell viability. Neuronal levels of casp3 were elevated in response to 6 h high glucose compared to normal glucose. Treatment of DRG with scrambled miRNA increased casp3 activation under both normal and high glucose conditions, indicating some damage occurred from the lentiviral infection. Neurons treated with Drp1 miRNA showed a decrease in casp3 compared to lentivirus control vector infection. These data were corroborated using 20 μM of the specific Drp1 chemical inhibitor mdiv-1 [34], demonstrating that chemical inhibition of Drp1 reduces expression of casp3 in response to high glucose exposure *in vitro* (data not shown).

Discussion

Previous work in our laboratory documented the role of oxidative stress and Mt dysregulation in type 1 and 2 rodent models and in cell culture models of DN [4, 6, 20, 28].

The current study extends these investigations by examining the impact of hyperglycemia on Mt networks *in vitro* and *in vivo* and the balance between Mt biogenesis and Mt fission. Here we demonstrate (a) increased Mt biogenesis *in vivo* and *in vitro* i.e. an increase in measures of MtDNA replication; (b) an increase in Mt fission with continued hyperglycemia, as assessed by an increase in number of Mt in neurons from mice with DN, these Mt are small and fragmented with a cristae pattern that indicates dysfunction; and (c) that blocking Mt fission in a short term model of hyperglycemic-mediated injury promotes neuronal survival. Our results suggest that neurons initially respond to hyperglycemia by enhancing both Mt biogenesis and Mt fission, but over time and with the accumulation of ROS, the balance favors Mt fission producing small aberrant Mt with reduced respiratory capacity.

Mt networks are dynamic and respond to external signals by increasing the actual mass of the network (biogenesis) as well as dispersing the existing Mt into a larger network (fission). This was explored by examining both Mt biogenesis and fission in the sciatic nerve of diabetic (BKS-db/db) and non-diabetic (db/+) mice. Whole nerve microarray studies [26] of MtDNA indicate Mt biogenesis occurs in mice with DN and previous studies link Mt biogenesis with Mt increased metabolic load[35, 36]. We detected an increase in MtDNA indicative of Mt biogenesis following 20 weeks of diabetes in the BKS-db/db mice. An increase in Mt mass is also supported by the increased expression of Mt specific COX-IV mRNA and protein. Up-regulation of Mt biogenesis as a means to accommodate the elevated glucose load is consistent with our hypothesis that neurons under hyperglycemic conditions are subjected to metabolism-induced oxidative stress [37, 38]. In NT2 cells, a model system for CNS neurons, increased Mt biogenesis is correlated with a reduction in Mt oxidative stress [38]. Similarly, promotion of Mt biogenesis in endothelial cells prevented hyperglycemia-induced oxidative stress [39]. These studies demonstrate a connection between Mt biogenesis and the capacity to handle metabolic load. Our investigations demonstrate that in peripheral sensory neurons, Mt biogenesis is activated in response to diabetes. We propose that Mt biogenesis is acting as a defense mechanism in response to hyperglycemia-induced stress in diabetic DRG neurons

A coordinate and/or alternative response to an increase in metabolic load is Mt fission. This strategy is frequently used by neurons under increased physiological stress. Increased Mt fission is essential in hippocampal neurons, which require active Mt fission for formation, function, and maintenance of synapses, processes that place a higher metabolic demand on neurons [8, 40]. In DRG neurons, Mt biogenesis likely acts as a protective mechanism against glucotoxicity; however, over time, the cell exhausts this capacity resulting in Mt fission without replication of MtDNA. In the DRG of the BKS-db/db, 20 weeks of diabetes induces an increase in the number of Mt but a marked decrease in Mt size, indicating an increase rate of Mt fission. These data suggest that the Mt biogenesis occurring in diabetic neurons is insufficient to produce healthy Mt that the balance is towards Mt fission and that continued fission results in aberrant Mt morphology. Damaged Mt demonstrate altered morphology, breakdown of cristae and loss of function [4, 25, 41-43]. Changes in Mt morphology are classified into five categories, progressing from “normal” to “vesicular” to “swollen”, with “swollen” coinciding with the beginning stages of cell death [31]. Our data

document increased numbers of Mt with dysfunctional morphology corresponding to the intermediate stages of cell damage, normal-vesicular and vesicular. The increased density (darkened appearance) of the Mt matrix indicates that Mt have decreased electron transport complex activity. Taken together, our findings show *in vivo* diabetic neurons undergo a) Mt biogenesis, albeit insufficient; b) Mt morphological changes, and c) Mt biochemical dysfunction.

To further explore the effects of hyperglycemia on Mt biogenesis and fission in neurons, DRG neurons were exposed to high glucose media *in vitro.* DRG neurons exhibited a significant increase in MtDNA; however, no change in Mt specific proteins, such as COX-IV, was detected. The increase in MtDNA without simultaneous increase in Mt protein is likely due to a combination of oxidative stress and temporal effects. Low levels of oxidative stress increase MtDNA copy number, whereas excess oxidative stress is shown to damage and inhibit Mt biogenesis [44]. The lack of detectable increase in Mt-encoded proteins is potentially due to insufficient time for Mt protein translation following DNA replication, or that the Mt translation machinery is damaged by hyperglycemia-induced oxidative stress. Our previous studies of hyperglycemic-induced oxidative stress reveal a biphasic response with early (up to 6 h) and late (after 12 h) changes in gene and protein expression [4]. Further studies comparing the timing of the antioxidant response and Mt biogenesis and fission are under way to clarify this issue.

The increased number of Mt and their diminished size indicate that Mt fission, a component of Mt biogenesis, may be overactive in diabetic neurons. Regulation of the fission protein Drp1 *in vivo* and *in vitro* supports this idea. We hypothesized that depletion of Drp1 in embryonic DRG neurons would lead to increased viability. Depletion of Drp1 by miRNA had a rescue effect on short-term neuronal glucotoxicity, as indicated by diminished cleaved Caspase-3. Thus, in vitro, we found that inhibition of Drp1 diminished hyperglycemia mediated cellular dysfunction. Further confirmation for this idea comes from recent reports of altered Drp1 levels in cortical neurons from Alzheimer's disease that correspond to changes in neuronal Mt number and distribution [45]. Previous work has also shown that dysfunction in the fission-fusion machinery leads to inherited neuropathies [46, 47] and that inhibition of Drp1 renders cells resistant to dysfunction [32]. Collectively, these studies demonstrate the importance of the fission-fusion machinery in neuronal dysfunction and implicate imbalances in the fission-fusion machinery in the pathogenesis of DN. Furthermore, Drp1 is in part regulated by post-translational modifications, which facilitate cellular distribution and/or stability of Drp1, important to promote fission [48-50]

In summary, our findings suggest an increase in Mt biogenesis and fission in response to hyperglycemia in both *in vivo* and *in vitro* models of DN. While Mt numbers increase in neurons from diabetic mice, these Mt are small with a dysfunctional morphology, suggesting an excessive upregulation of Mt fission. Knockdown of Drp1, a key regulator of Mt fission, rescues Mt from short-term glucotoxicity *in vitro*. Despite the short-term beneficial effects of Drp1 knockdown, its role in the long-term development of diabetic neuropathy remains to be defined. Further studies are currently underway to dissect the role of Mt biogenesis and fission events in glucotoxicity and to determine the efficacy of site-directed *in vivo* knockdown of Drp1 in supporting neuronal survival in diabetic conditions.

Acknowledgments

We would like to thank Ms. Judith Boldt for her expert secretarial assistance, Dr. Kelli Sullivan for careful reading of the text, and Kristine M. Haines for assistance with BrdU signal analysis. This work was supported by National Institute of Health T32 D07245, the Juvenile Diabetes Research Foundation Center for the Study of Complications in Diabetes, the Program for Neurological Research and Development (PNRD) and the A. Alfred Taubman Medical Research Institute. This work utilized the Morphology and Image Analysis Core of the Michigan Diabetes Research and Training Center funded by NIH5P60 DK20572 and U01DK076137 from the National Institute of Diabetes & Digestive & Kidney Diseases.

Abbreviations

BrdU	bromodeoxyuridine
casp3	cleaved Caspase-3
DN	diabetic neuropathy
DRG	dorsal root ganglion
Drp1	dynamin-related protein 1
Mt	Mitochondrial or mitochondria
MFN2	mitofusin 2
COX-IV	OxPhos Complex IV subunit I
PGC-1α	peroxisome proliferator activated receptor-coactivator alpha
ROS	reactive oxygen species

References

[1]. Leinninger GM, Backus C, Sastry AM, Yi YB, Wang CW, Feldman EL. Mitochondria in DRG neurons undergo hyperglycemic mediated injury through Bim, Bax and the fission protein Drp1. Neurobiology of disease. 2006; 23:11–22. [PubMed: 16684605]

[2]. Cartoni R, Martinou JC. Role of mitofusin 2 mutations in the physiopathology of Charcot-Marie-Tooth disease type 2A. Exp Neurol. 2009; 218:268–273. [PubMed: 19427854]

[3]. Martin CL, Albers J, Herman WH, et al. Neuropathy among the diabetes control and complications trial cohort 8 years after trial completion. Diabetes care. 2006; 29:340–344. [PubMed: 16443884]

[4]. Vincent AM, McLean LL, Backus C, Feldman EL. Short-term hyperglycemia produces oxidative damage and apoptosis in neurons. FASEB J. 2005; 19:638–640. [PubMed: 15677696]

[5]. Huang TJ, Price SA, Chilton L, et al. Insulin prevents depolarization of the mitochondrial inner membrane in sensory neurons of type 1 diabetic rats in the presence of sustained hyperglycemia. Diabetes. 2003; 52:2129–2136. [PubMed: 12882932]

[6]. Vincent AM, Stevens MJ, Backus C, McLean LL, Feldman EL. Cell culture modeling to test therapies against hyperglycemia-mediated oxidative stress and injury. Antioxid Redox Signal. 2005; 7:1494–1506. [PubMed: 16356113]

[7]. Russell JW, Golovoy D, Vincent AM, et al. High glucose-induced oxidative stress and mitochondrial dysfunction in neurons. Faseb J. 2002; 16:1738–1748. [PubMed: 12409316]

[8]. Berman SB, Pineda FJ, Hardwick JM. Mitochondrial fission and fusion dynamics: the long and short of it. Cell death and differentiation. 2008; 15:1147–1152. [PubMed: 18437161]

[9]. Tatsuta T, Langer T. Quality control of mitochondria: protection against neurodegeneration and ageing. The EMBO journal. 2008; 27:306–314. [PubMed: 18216873]

[10]. Rasbach KA, Schnellmann RG. Signaling of mitochondrial biogenesis following oxidant injury. The Journal of biological chemistry. 2007; 282:2355–2362. [PubMed: 17116659]

[11]. Lopez-Lluch G, Hunt N, Jones B, et al. Calorie restriction induces mitochondrial biogenesis and bioenergetic efficiency. Proceedings of the National Academy of Sciences of the United States of America. 2006; 103:1768–1773. [PubMed: 16446459]

[12]. Cohen HY, Miller C, Bitterman KJ, et al. Calorie restriction promotes mammalian cell survival by inducing the SIRT1 deacetylase. Science (New York, NY. 2004; 305:390–392.

[13]. St-Pierre J, Drori S, Uldry M, et al. Suppression of reactive oxygen species and neurodegeneration by the PGC-1 transcriptional coactivators. Cell. 2006; 127:397–408. [PubMed: 17055439]

[14]. Li H, Chen Y, Jones AF, et al. Bcl-xL induces Drp1-dependent synapse formation in cultured hippocampal neurons. Proceedings of the National Academy of Sciences of the United States of America. 2008; 105:2169–2174. [PubMed: 18250306]

[15]. Smirnova E, Shurland DL, Ryazantsev SN, van der Bliek AM. A human dynamin-related protein controls the distribution of mitochondria. J Cell Biol. 1998; 143:351–358. [PubMed: 9786947]

[16]. Zhu PP, Patterson A, Stadler J, Seeburg DP, Sheng M, Blackstone C. Intra- and intermolecular domain interactions of the C-terminal GTPase effector domain of the multimeric dynamin-like GTPase Drp1. J BiolChem. 2004; 279:35967–35974.

[17]. James DI, Parone PA, Mattenberger Y, Martinou JC. hFis1, a novel component of the mammalian mitochondrial fission machinery. J BiolChem. 2003; 278:36373–36379.

[18]. Lee YJ, Jeong SY, Karbowski M, Smith CL, Youle RJ. Roles of the mammalian mitochondrial fission and fusion mediators Fis1, Drp1, and Opa1 in apoptosis. Molecular biology of the cell. 2004; 15:5001–5011. [PubMed: 15356267]

[19]. Yoon Y, Krueger EW, Oswald BJ, McNiven MA. The mitochondrial protein hFis1 regulates mitochondrial fission in mammalian cells through an interaction with the dynamin-like protein DLP1. MolCell Biol. 2003; 23:5409–5420.

[20]. Sullivan KA, Hayes JM, Wiggin TD, et al. Mouse models of diabetic neuropathy. Neurobiology of disease. 2007; 28:276–285. [PubMed: 17804249]

[21]. Mayfield J. Diagnosis and classification of diabetes mellitus: new criteria. Am FamPhysician. 1998; 58:1355–1370.

[22]. Sullivan KA, Lillie JH, Greene DA. Digital electron microscopic analysis of regenerating axon clusters in human sural nerve biopsies. Society for Neuroscience Abstracts. 1996; 24.17:37.

[23]. Kim B, Leventhal PS, Saltiel AR, Feldman EL. Insulin-like growth factor-I-mediated neurite outgrowth in vitro requires MAP kinase activation. Journal of Biological Chemistry. 1997; 272:21268–21273. [PubMed: 9261137]

[24]. Kim B, Oh SS, van Golen CM, Feldman EL. Differential regulation of insulin receptor substrate-1 degradation during mannitol and okadaic acid induced apoptosis in human neuroblastoma cells. Cellular Signalling. 2004; 17:769–775. [PubMed: 15722201]

[25]. Vincent AM, Russell JW, Low P, Feldman EL. Oxidative stress in the pathogenesis of diabetic neuropathy. Endocrine reviews. 2004; 25:612–628. [PubMed: 15294884]

[26]. Wiggin TD, Kretzler M, Pennathur S, Sullivan KA, Brosius FC, Feldman EL. Rosiglitazone Treatment Reduces Diabetic Neuropathy in STZ Treated DBA/2J Mice. Endocrinology. 2008

[27]. Howarth FC, Jacobson M, Shafiullah M, Adeghate E. Long-term effects of streptozotocin-induced diabetes on the electrocardiogram, physical activity and body temperature in rats. Exp Physiol. 2005; 90:827–835. [PubMed: 16091403]

[28]. Sullivan KA, Lentz SI, Roberts JL Jr. Feldman EL. Criteria for creating and assessing mouse models of diabetic neuropathy. Curr Drug Targets. 2008; 9:3–13. [PubMed: 18220709]

[29]. Mattingly KA, Ivanova MM, Riggs KA, Wickramasinghe NS, Barch MJ, Klinge CM. Estradiol stimulates transcription of nuclear respiratory factor-1 and increases mitochondrial biogenesis. Molecular endocrinology (Baltimore, Md. 2008; 22:609–622.

[30]. Lelliott CJ, Ljungberg A, Ahnmark A, et al. Hepatic PGC-1beta overexpression induces combined hyperlipidemia and modulates the response to PPARalpha activation. Arteriosclerosis, thrombosis, and vascular biology. 2007; 27:2707–2713.

[31]. Sun MG, Williams J, Munoz-Pinedo C, et al. Correlated three-dimensional light and electron microscopy reveals transformation of mitochondria during apoptosis. Nature cell biology. 2007; 9:1057–1065.

[32]. Frank S, Gaume B, Bergmann-Leitner ES, et al. The role of dynamin-related protein 1, a mediator of mitochondrial fission, in apoptosis. DevCell. 2001; 1:515–525.

[33]. Karbowski M, Lee YJ, Gaume B, et al. Spatial and temporal association of Bax with mitochondrial fission sites, Drp1, and Mfn2 during apoptosis. Journal of Cell Biology. 2002; 159:931–938. [PubMed: 12499352]

[34]. Cassidy-Stone A, Chipuk JE, Ingerman E, et al. Chemical inhibition of the mitochondrial division dynamin reveals its role in Bax/Bak-dependent mitochondrial outer membrane permeabilization. Developmental cell. 2008; 14:193–204. [PubMed: 18267088]

[35]. Powelka AM, Seth A, Virbasius JV, et al. Suppression of oxidative metabolism and mitochondrial biogenesis by the transcriptional corepressor RIP140 in mouse adipocytes. J Clin Invest. 2006; 116:125–136. [PubMed: 16374519]

[36]. Haden DW, Suliman HB, Carraway MS, et al. Mitochondrial biogenesis restores oxidative metabolism during Staphylococcus aureus sepsis. American journal of respiratory and critical care medicine. 2007; 176:768–777. [PubMed: 17600279]

[37]. Bogacka I, Ukropcova B, McNeil M, Gimble JM, Smith SR. Structural and functional consequences of mitochondrial biogenesis in human adipocytes in vitro. J ClinEndocrinolMetab. 2005; 90:6650–6656.

[38]. Ghosh S, Patel N, Rahn D, et al. The thiazolidinedione pioglitazone alters mitochondrial function in human neuron-like cells. Molecular pharmacology. 2007; 71:1695–1702. [PubMed: 17387142]

[39]. Kukidome D, Nishikawa T, Sonoda K, et al. Activation of AMP-activated protein kinase reduces hyperglycemia-induced mitochondrial reactive oxygen species production and promotes mitochondrial biogenesis in human umbilical vein endothelial cells. Diabetes. 2006; 55:120–127. [PubMed: 16380484]

[40]. Li Z, Okamoto K, Hayashi Y, Sheng M. The importance of dendritic mitochondria in the morphogenesis and plasticity of spines and synapses. Cell. 2004; 119:873–887. [PubMed: 15607982]

[41]. Tinari A, Garofalo T, Sorice M, Esposti MD, Malorni W. Mitoptosis: different pathways for mitochondrial execution. Autophagy. 2007; 3:282–284. [PubMed: 17329965]

[42]. James AM, Murphy MP. How mitochondrial damage affects cell function. Journal of biomedical science. 2002; 9:475–487. [PubMed: 12372986]

[43]. Brownlee M. Biochemistry and molecular cell biology of diabetic complications. Nature. 2001; 414:813–820. [PubMed: 11742414]

[44]. Lee HC, Wei YH. Mitochondrial biogenesis and mitochondrial DNA maintenance of mammalian cells under oxidative stress. Int J Biochem Cell Biol. 2005; 37:822–834. [PubMed: 15694841]

[45]. Wang X, Su B, Lee HG, et al. Impaired balance of mitochondrial fission and fusion in Alzheimer's disease. J Neurosci. 2009; 29:9090–9103. [PubMed: 19605646]

[46]. Alexander C, Votruba M, Pesch UE, et al. OPA1, encoding a dynamin-related GTPase, is mutated in autosomal dominant optic atrophy linked to chromosome 3q28. NatGenet. 2000; 26:211–215.

[47]. Bette S, Schlaszus H, Wissinger B, Meyermann R, Mittelbronn M. OPA1, associated with autosomal dominant optic atrophy, is widely expressed in the human brain. Acta neuropathologica. 2005; 109:393–399. [PubMed: 15700187]

[48]. Santel A, Frank S. Shaping mitochondria: The complex posttranslational regulation of the mitochondrial fission protein DRP1. IUBMB Life. 2008; 60:448–455. [PubMed: 18465792]

[49]. Uo T, Dworzak J, Kinoshita C, et al. Drp1 levels constitutively regulate mitochondrial dynamics and cell survival in cortical neurons. Exp Neurol. 2009; 218:274–285. [PubMed: 19445933]

[50]. Figueroa-Romero C, Iniguez-Lluhi JA, Standler J, et al. SUMOylation of the mitochondrial fission protien Drp1 occurs at multiple nonconsensus sites with the B domain and is linked to its activity cycle. The FASEB Journal. 2009 in press.

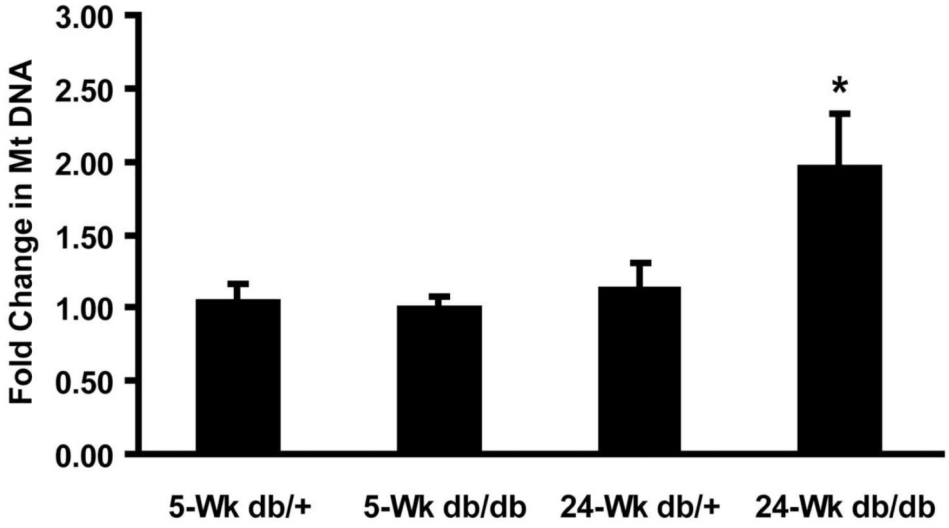

Fig. 1. Mitochondrial DNA levels increase in diabetic mice

Mitochondrial (Mt) DNA levels were determined by measuring cytochrome c DNA levels. Genomic DNA isolated from control (db/+) and diabetic (db/db) DRG neurons at 5 and 24 wk was subjected to real-time (RT) PCR using primers listed in table 1 ($n = 4$). * $p < 0.05$.

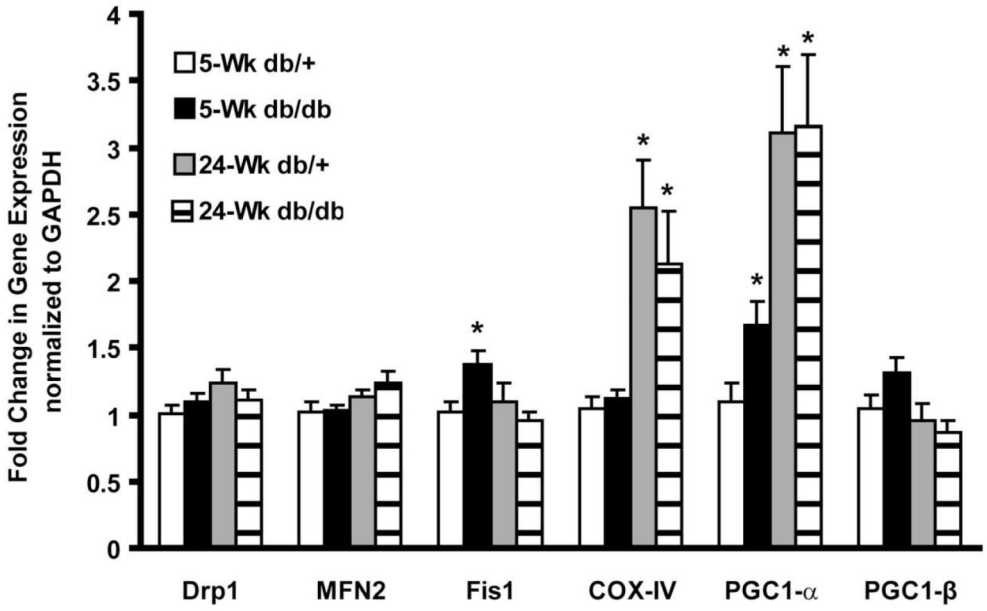

Fig. 2. Transcription of genes involved in mitochondria biogenesis is significantly increased in response to an acute response to hyperglycemia

RNA was extracted from DRG of control (db/+) and diabetic (db/db) mice at 5 and 24 wk of age. RT-PCR was used to analyze mRNA levels of genes involved in Mt biogenesis (PGC1-α, PGC1-β), Mt fission (Drp1 and Fis1), Mt fusion (MFN2) and Mt mass (COX-IV).

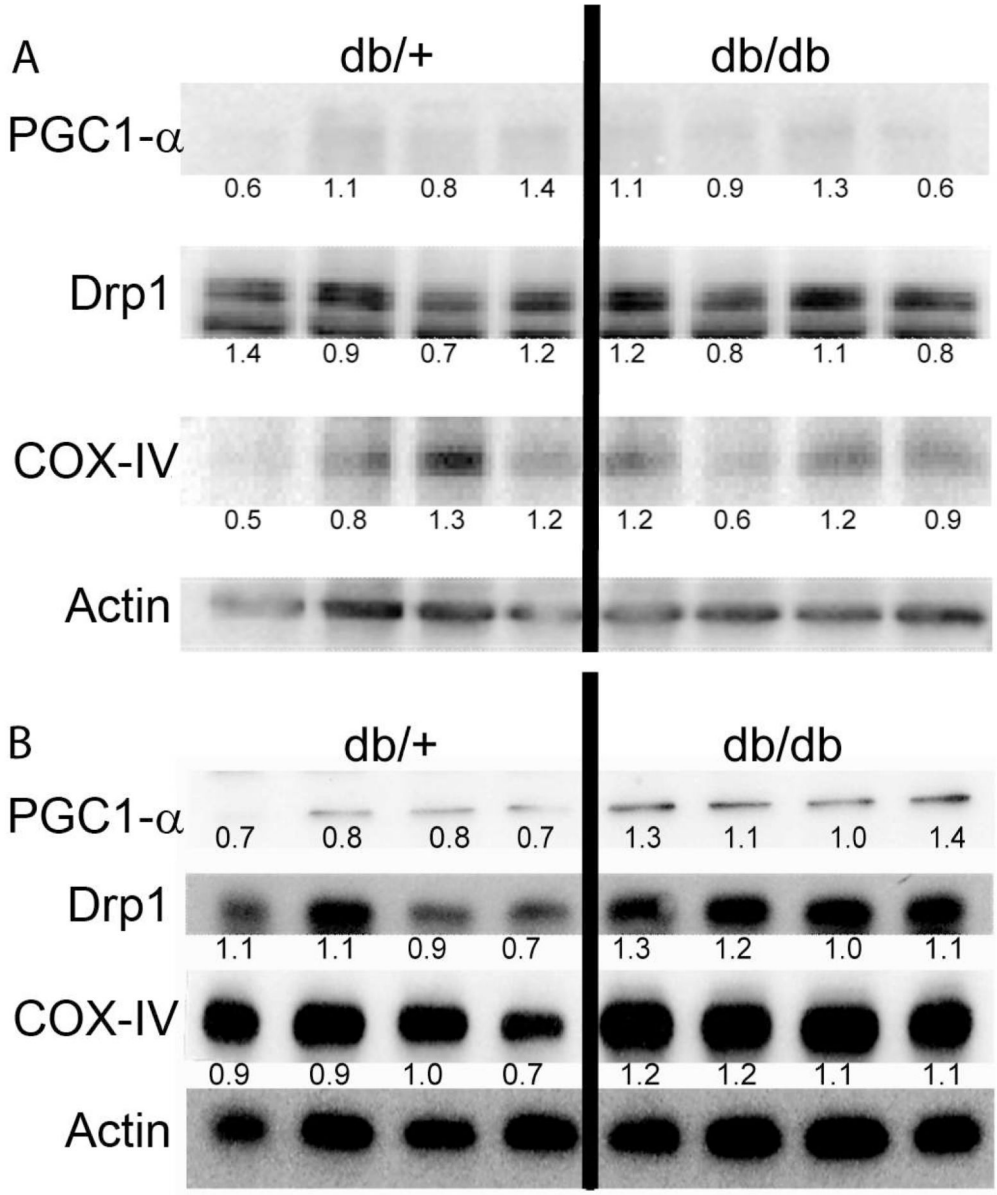

Fig. 3. Prolonged hyperglycemia significantly increases protein levels of PGC1-α, COX-IV, and Drp1

Immunoblot of mitochondrial proteins from DRG neurons of 5 wk (A) and 24 wk (B) control (db/+) and diabetic (db/db) mice. The blots were analyzed using antibodies against PGC1-α, Drp1, COX-IV and actin. Each lane represents DRG lysates from different animals. Numbers beneath bands indicate density relative to actin.

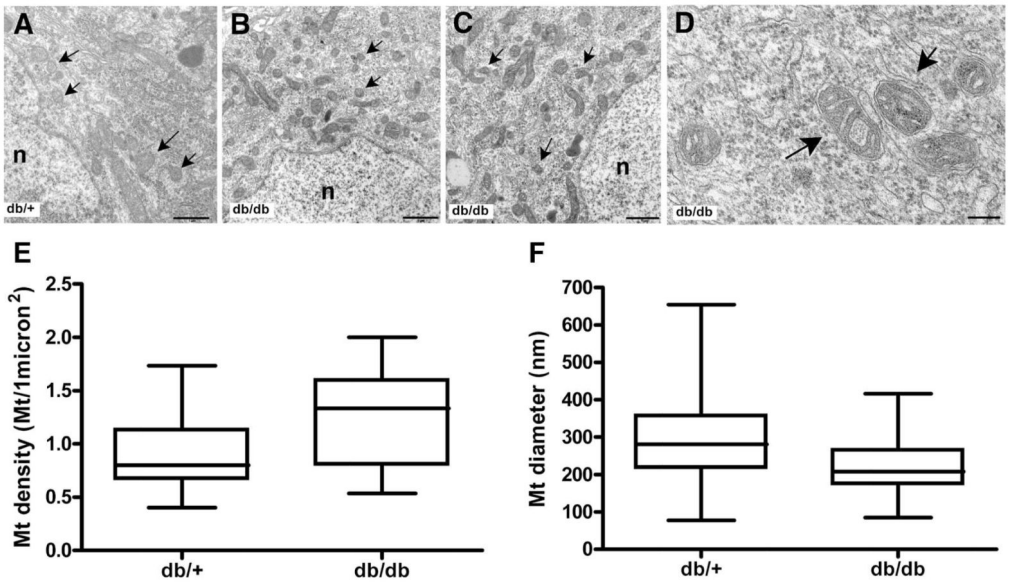

Fig. 4. Hyperglycemia leads to altered mitochondria dynamics and morphology in DRG neurons *in vivo*

Transmision electron micrographs of Mt from control (A) and diabetic neurons (B, C and D). Arrows indicate mitochondria. (D) Mitochondria from DRG neuron from diabetic (db/db) mice show slightly dilated intracristal space while the matrix is still dense. n, nucleus. Scale bar: A, B and C = 1 μm; D = 180 nm. (E) Quantitative analysis of mitochondria in DRG neurons from 24 wk old mice showed an increase in the number of Mt in the diabetic (db/db) compared to control (db/+) mice; $p < 0.0001$. (F) Mitochondria from diabetic (db/db) mice showed reduced diameters compared to control (db/+); $p < 0.0001$. n=2

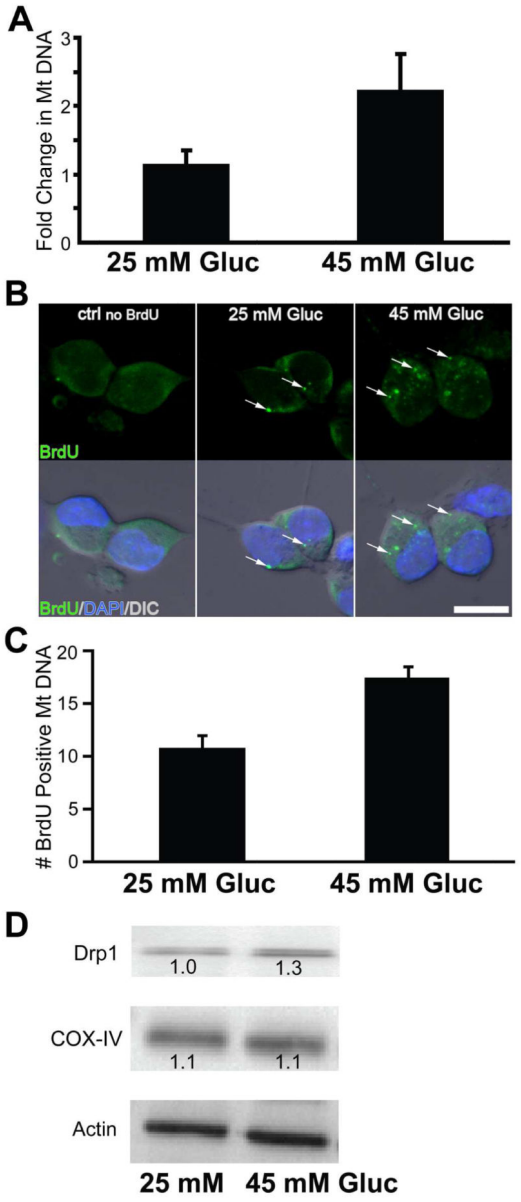

Fig. 5. Hyperglycemia increases mitochondrial biogenesis and fission in DRG neurons *in vitro*

(A) DRG. Dissected and dissociated rat E15 DRGs were incubated in the presence of control (25 mM) or high glucose media (45 mM) for 6 h. Quantitation of cytochorome b DNA was used as a marker for MtDNA. n=3 (B) *In vitro* analysis of BrdU incorporation into MtDNA of DRG neurons under hyperglycemia. DRG neurons were cultured in the presence (or absence, ctrl no BrdU) of BrdU and normal (25 mM) or high glucose (45 mM) for 6 h. BrdU incorporation into MtDNA (arrows) was visualized by immunocytochemstry with tyramide amplified AlexaFluor 488 green signal (top panels) and merged with nuclear staining (DAPI, blue) and differential interference contrast (DIC) images (lower panels). Cells were visualized using an Olympus FluoView 500 laser scanning confocal microscope. Bar = 10 μm. (C) Quantitation of MtDNA was done by identifying BrdU-positive DRG soma. *In vitro* cultures were incubated in control or high glucose media for 6 h. n=10 per group (D) Western blot analysis of *in vitro* cultures DRG after control or treatment media exposure. Protein lysates were subjected to SDS-PAGE and analyzed with antibodies against COX-IV, Drp1, and actin (internal control).

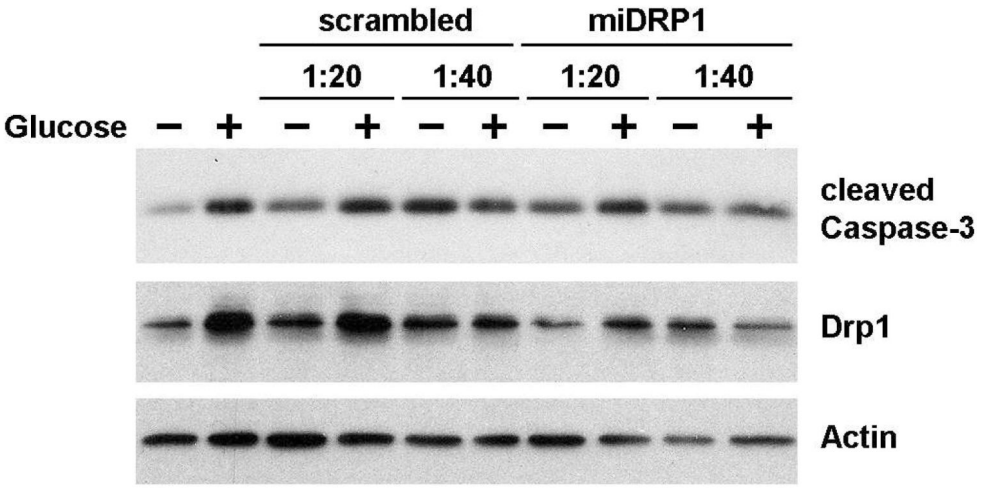

Fig. 6. Drp1 promotes hyperglycemia-induced cell death in sensory neurons

Cultured Rat E15 DRG neurons were lentiviral infected (1:20 or 1:40 dilution) with non-specific miRNA (scrambled), Drp1 specific miRNA (mouse), or non-infected (control). Neurons were treated with high glucose (+) or control (-) media. Cell extracts were subjected to SDS-PAGE and analyzed by western blotting with antibodies for cleaved Caspase-3, Drp1 and actin (internal control).

Table 1

Sequences for Mt DNA quantification

Target Gene	Primer Sequence (5′ - 3′)
Rat	Sense: GGC TAT GTA CTC CCA TGA GGA C
Cytochrome b	Antisense: CCT CCT CAG ATT CAT TCG AC
Rat	Sense: ATC ATG TTT GAG ACC TTC AAC ACC C
Actin	Antisense: CAT CTC TTG CTC GAA GTC TAG G
Mouse	Sense: GGC TAC GTC CTT CCA TGA GGA C
Cytochrome b	Antisense: GAA GCC CCC TCA AAT TCA TTC GAC
Mouse	Sense: CAT CTC CTG CTC GAA GTC TAG
Actin	Antisense: ATC ATG TTT GAG ACC TTC AAC ACC C

Table 2

Sequences of primers for real-time PCR

Target Gene	Primer Sequence (5′ - 3′)
GAPDH	Sense: AGT ATG TCG TGG AGT CTA CTG GTG Antisense: TGA GTT GTC ATA TTT CTC GTG GTT
Drp1	Sense: AGG TGG CCT TAA CAC TAT TGA CA Antisense: AGA CGC TTA ATC TGA CGT TTG AC
MFN2	Sense: CTC AAG ACT ACA AGC TGC GAA TTA Antisense: GGT ACT CGT CAA CTA GCA CAG AGA
Fis1	Sense: CGA AGC AAA TAC AAT GAG GAC A Antisense: TCA TAT TCC TTG AGC CGG TAG T
COX-IV	Sense: TCA TAG CAG GAT TTG TTC ACT GAT Antisense: AAG AGA CAG TGT TTC ATG TGG TGT
PGC1-α	Sense: CTG TAT GGA GTG ACA TAG AGT GTG C Antisense: GAA AGC TGT CTG TAT CCA AGT CAT T
PGC1-β	Sense: ACA TTC GAA ATC TCT CCA GTG AC Antisense: GCT TCT GGC CTC TTT TAC TTC TC